Article

Journal of Industrial Textiles

2022, Vol. 51(4S) 5910S–5937S

DOI: 10.1177/1528083720971344
journals.sagepub.com/home/jit
SAGE

# Mechanical, water absorption and wear characteristics of novel polymeric composites: Impact of hybrid natural fibers and oil cake filler addition

**KR Sumesh[1], V Kavimani[2], G Rajeshkumar[3], S Indran[4] and Anish Khan[5]**

## Abstract

A novel epoxy-based composites were fabricated by reinforcing pineapple/flax (PF) fibers and peanut oil cake (PCF) filler using the hand layup cum compression moulding technique and investigated its mechanical, water absorption and wear properties as a function of wt.% of PF fibers (20–40 wt.%) and PCF (1–3 wt.%). The XRD and FTIR results proved the presence of lignocellulosic nature in PCF. Mechanical test results showed significant enhancement in the properties after the addition of PCF. The maximum tensile, flexural and impact properties of 37. 89 MPa, 70.28 MPa and 96.99 J/m were observed in the composites having 20 wt.% of PF and 2 wt.% of PCF. Taguchi based optimization observed a lower specific wear rate (SWR) with 2 wt.% PCF/20 wt.% PF/5

[1]Department of Mechanical Engineering, KPR Institute of Engineering and Technology, Coimbatore, India
[2]Department of Mechanical Engineering, Karpagam Academy of Higher Education, Coimbatore, India
[3]Department of Mechanical Engineering, PSG Institute of Technology and Applied Research, Coimbatore, India
[4]Department of Mechanical Engineering, Rohini College of Engineering & Technology, Kanyakumari, India
[5]Center of Excellence for Advanced Materials Research, Chemistry Department, Faculty of Science, King Abdulaziz University, Jeddah, Saudi Arabia

**Corresponding author:**
KR Sumesh, Department of Mechanical Engineering, KPR Institute of Engineering and Technology, Arasur, Coimbatore 641407, Tamilnadu, India.
Email: sumesh2311@gmail.com

N load and 1500 m sliding distance (SD) combination. The ANOVA results proved the significance of PCF, PF fiber, sliding distance, and load for SWR in this experimentation. The Taguchi optimized results observed a lower coefficient of friction (COF) in 2 wt.% PCF/20 wt.% PF/5N load/500 m SD combination. SEM results displayed surface deformations in the wear-tested composites.

**Keywords**
Pineapple fiber, flax fiber, peanut oil cake filler, mechanical properties, wear, Taguchi optimization

## Introduction

The world is facing a major issue in disposing of various solid wastes generated from our daily life. The disposing of plastics has become a vital issue due to its harmful effect causing air, water, and soil pollution. The natural wastes or biodegradable wastes utilization and management is the perfect solution for this excessive non-biodegradable plastic usage [1–3]. In this context, the natural fibers like kenaf, jute, ramie, flax, leaves of pineapple, sisal, banana, seeds of kapok, and coir have been utilized as the reinforcements for producing composites for industrial and automobile applications. The high availability, low pollution-causing substance, comparable mechanical properties, and low cost attracted the composite industries and researchers to this field [4–7].

Natural fibers have been combined with different thermoset and thermoplastic matrix for the specific applications. These fibers growing in the soil are hydrophilic in nature; which is not adhere appropriately with hydrophobic resin. Surface treatments using NaOH, potassium permanganate, silane, stearic acid, benzoyl peroxide treatments are the best solution for enhancing the fiber/matrix bonding and improving the water resistance property [8–10]. A literature mentioned that pineapple fiber (30 wt.%) incorporation increased the tensile strength of the polymeric composites and NaOH treatment improved the compatibility of fiber/resin with low fracture surface and supports to enhance the properties of polymer-based composites further [11]. In another work, pineapple fiber substitution up to 45 wt.% enhanced the mechanical and structural properties of the polymer matrix composite [12].

Cellulosic nature structure in fiber controlled the frictional properties of flax-based composites. In addition to this, the contact area and applied load are the significant factors influencing the tribological behavior of natural fiber based composites [13]. Moreover, in the flax fiber (at 40 wt.%) reinforced polypropylene composite the tribological characteristics were influenced by the fiber orientation [14]. Hybridization of flax/basalt above 40 wt.% showed structural abnormality with more fracture surface, producing lesser mechanical properties in natural fiber composites [15].

Bamboo based epoxy composites showed good wear resistance at higher sliding distance conditions and it does not have much influence of the increase in sliding velocity [16]. Reinforcement substitution of oil palm and kenaf fibers in a higher weight percentage up to 70% showed reduction in wear applications of epoxy matrix composites. Wear cracks, debonding surfaces, fiber breakages, grooves were observed in severe rate due to poor bonding characteristics of fiber/matrix phase [17]. Wear loss was reduced by adding *Hibiscus sabdariffa* fiber in urea-formaldehyde polymer composites [18]. The addition of jute, *Grewia optiva*, short wood, *Musaceae*, betelnut fibers were also a contender to the composites wear-resistant properties [19–23].

Apart from fiber reinforcement, the incorporation of fillers like $Al_2O_3$, $TiO_2$, and oil cake are also supported to enhance the properties of epoxy-based composites [24–26]. The incorporation of hybrid natural fibers up to 35 wt.%, oil cake filler from 1–3 wt.% improved the mechanical properties of epoxy based composites [26]. Tribological behaviour of composites were enhanced by adding fillers of jute, titanium oxide, solid glass microspheres, jatropha oil cake, and Multi-Wall Carbon Nano Tube (MWCNT) to the composites [27–30]. Interaction of graphene and polyvinyl alcohol were enhanced by jute and MWCNT fillers that reduce the wear loss of the composites [27].

Response surface methodology was adopted to optimize the short hair fiber addition in epoxy matrix composites. ANOVA table showed fiber substitution, applied load, sliding velocity, and sliding distance are the significant factors influencing wear characteristics of the composite [28]. Taguchi optimization using L27 trials was employed for finding hybrid fiber and operating parameters influencing the wear rate of the epoxy polymer matrix composites. The results showed 4 wt.% *Grewia optiva*/*Bauhinia vahlii* fiber combination with the sliding distance, velocity, and the load of 2000 m, 2.5 m/s, and 15 N as the optimized condition [22].

Optimization is vital in finding the best proportion of reinforcement, filler and other operating parameters for improving the tribological behavior of the natural fiber composites. Most of the previous research work, highlighted the optimization dealing with operating parameters considered in the wear testing than the polymer composite specification. The present study aimed to characterize the mechanical, water absorption and wear properties of a novel Pineapple/Flax (PF) fibers and Peanut Oil Cake Filler (PCF) reinforced composites. Furthermore, the wear properties of the composites with optimized varying load, sliding distance, filler and the reinforcement wt. % were reported for the first time.

## Materials and methods

### Materials

The pineapple and flax fibers and peanut oil cake were collected from various locations in Coimbatore, Tamilnadu, India. The fiberous structure in peanut oil cake enhances the bonding nature of epoxy-based composites [26]. A ratio of 10:1 epoxy resin (LY556 grade) and hardener (HY951 grade) was taken as the matrix phase in this experimentation [24]. The selected fibers pineapple and flax have high cellulose content of 64.3 wt.% and 62.1 wt.% respectively (Table 1).

### Methods

Hybrid fibers of 10 mm in length and 20–40 wt.%, were used for composite fabrication. Peanut oil cake filler (PCF) varying from 1, 2 and 3 wt. % was incorporated with this combination for enhancing the properties. Initially, PCF was ball-milled (2 hours and 3 hours) by the using high energy ball milling machine (800 rpm; 3:1 ball to PCF ratio) for making fine powder (Figure 1). A total of 9 composite specimens were fabricated using this PF, and PCF combination with epoxy-based matrix; its details were shown in Table 2.

*Incorporation of PCF into epoxy matrix.* The PCF was added to the epoxy matrix by using the mechanical stirring and ultrasonication processes. Both the process was carried out up to 15 minutes effectively to reduce the air bubble in composites during the compression moulding process. This properly mixed PCF/epoxy matrix is poured into the compression mould die which contain chopped PF hybrid fibers. The hand layup-cum-compression technique were used to fabricate the specimen as per the ASTM standard for composite characterization.

## Experimental details

### FTIR and XRD testing

The presence of cellulose content in PCF was examined using the X Pert PRO model diffractometer range from 5° to 40°. Crystallinity Index (CI) showing the the crystalline nature of PCF was calculated using the Segal empirical method [32] (1). FTIR analysis was carried out to find the functional groups present in PCF.

**Table 1.** Properties of pineapple and flax fibers.

| Properties | Units | Pineapple fiber [26] | Flax Fiber [31] |
|---|---|---|---|
| Cellulose | % | 64.3 | 62.1 |
| Lignin | % | 25.7 | 26.9 |
| Wax | % | 0.184 | 0.166 |
| Ash | % | 1.48 | 1.36 |
| Moisture content | % | 8.09 | 9.12 |
| Density | $kg/m^3$ | 1506 | 1424 |
| Tensile strength | MPa | 184 | 168 |
| Young's modulus | GPa | 6.32 | 8.98 |
| Diameter | μm | 120–250 | 150–320 |

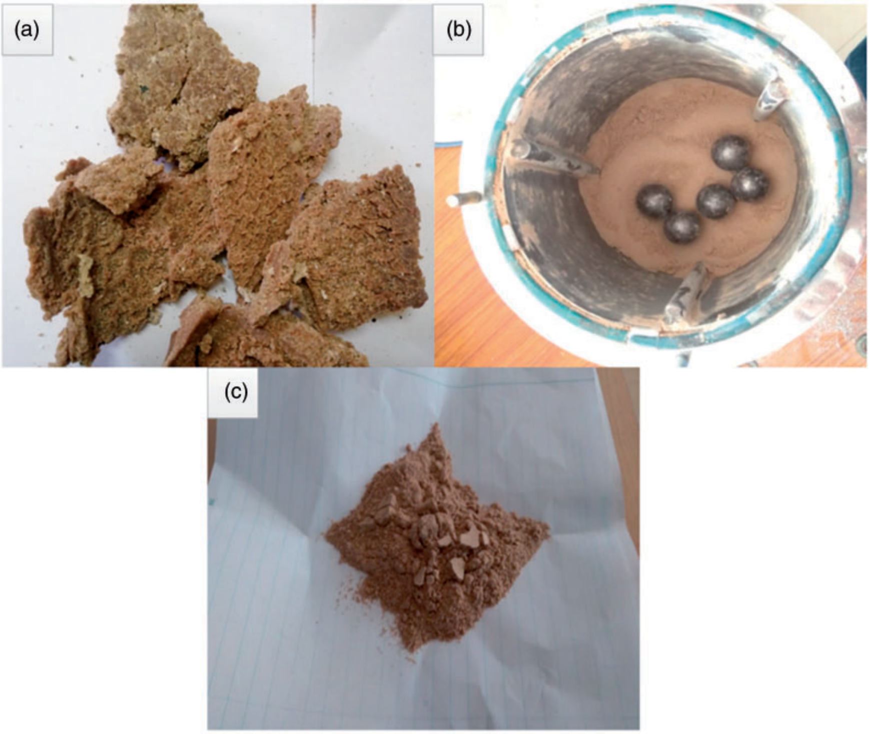


**Figure 1.** Filler reinforcement: (a) peanut oil cake, (b) ball milling of peanut oil cake, and (c) ball milled peanut oil cake filler.

**Table 2.** Combination of reinforcement used to fabricate hybrid composites.

| Designation | Combination of reinforcements |
|---|---|
| HC120 | 1 wt.% PCF / 20 wt.% PF |
| HC220 | 2 wt.% PCF / 20 wt.% PF |
| HC320 | 3 wt.% PCF / 20 wt.% PF |
| HC130 | 1 wt.% PCF / 30 wt.% PF |
| HC230 | 2 wt.% PCF / 30 wt.% PF |
| HC330 | 3 wt.% PCF / 30 wt.% PF |
| HC140 | 1 wt.% PCF / 40 wt.% PF |
| HC240 | 2 wt.% PCF / 40 wt.% PF |
| HC340 | 3 wt.% PCF / 40 wt.% PF |

Nexus 6800-50 machine was used with a wave number ranging from 400 $cm^{-1}$–4000 $cm^{-1}$, and the spectral resolution of 2 $cm^{-1}$.

$$\boldsymbol{CI} = \frac{\boldsymbol{I}_{200} - \boldsymbol{I}_{\boldsymbol{am}}}{\boldsymbol{I}_{200}} \times 100 \tag{1}$$

where, $I_{200}$ and $I_{am}$ represents the higher intensity peak and lower intensity peaks at various lattice planes [33]. The crystalline size (CrS) was computed using Scherer's equation (2) [34].

$$\boldsymbol{CrS} = \frac{\boldsymbol{K\lambda}}{\boldsymbol{\beta\cos\theta}} \tag{2}$$

where, 'K' stands for Scherer's constant which is equal to 0.89, '$\lambda$' denotes X ray wavelength with 0.154 nm, '$\beta$' represents Full width at half maximum range and '$\theta$' stands for Bragg angle.

## Mechanical testings

The universal testing machine (Tinius Olsen H10KL) was used to determine the tensile (ASTM D 638 - 17) and flexural (ASTM D790 - 17) strength of hybrid composites [35]. Impact strength followed ASTM D256 - 10(2018) with $6.5 \times 1.3 \times 0.3\,cm^3$ dimensions. The Izod impact test (ASTM D256 - 10(2018)) was carried out to estimate impact strength of the hybrid composites.

## Water absorption test

The water absorption test was carried out for ten days as per ASTM D570 - 98 (2018) standard. The size of the sample used for experimentation was $2 \times 2 \times 0.3\,cm^3$. Initially, the composites were dried in an oven, and the initial weight was taken. Then the specimens were dipped in water at room temperature, and changes in the mass were noted for every 24 h. Similarly, the readings were taken up to 10 days and the water absorption for the samples were computed by using the following equation (3). The fabricated specimen for mechanical and water absorption testing were shown in Figure 2.

$$\text{Water Absorption \%} = \frac{(\text{Wet Weight} - \text{Dry Weight})}{\text{Dry Weight}} \times 100 \tag{3}$$

## Wear testing

Linear reciprocating tribometer equipment (Figure 3) was employed to study the tribological characteristics of PCF/PF hybrid composite specimens. A chromium

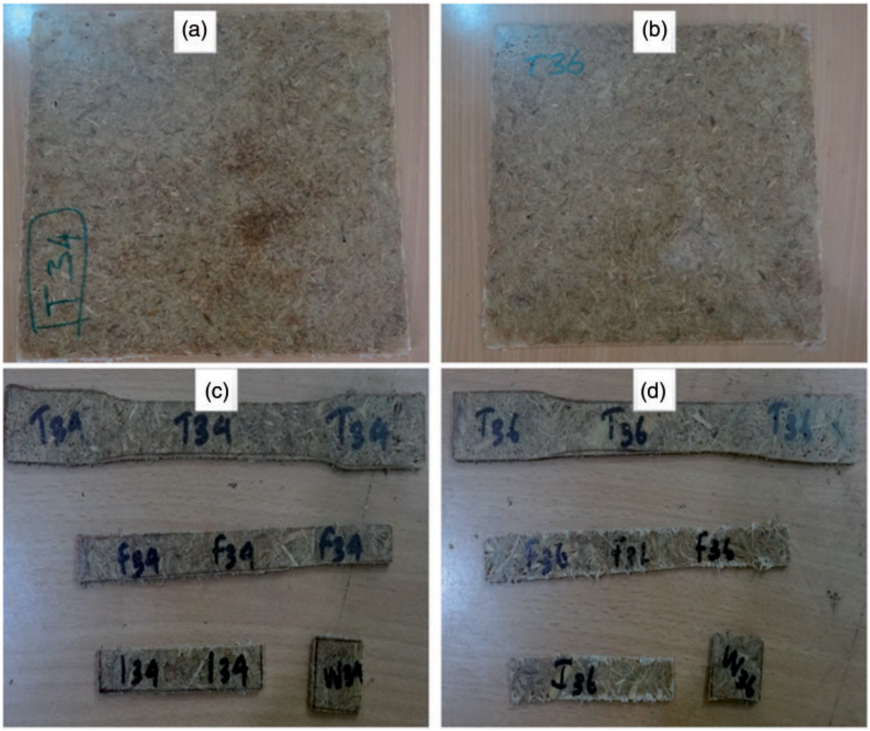


**Figure 2.** Fabricated samples for Tensile (T), Flexural (F), Impact (I) and Water absorption (W) tests having: (a), (c) 35 wt.% PF/2 wt.% PCF and (b), (d) 30 wt.% PF/2 wt.% PCF combinations.

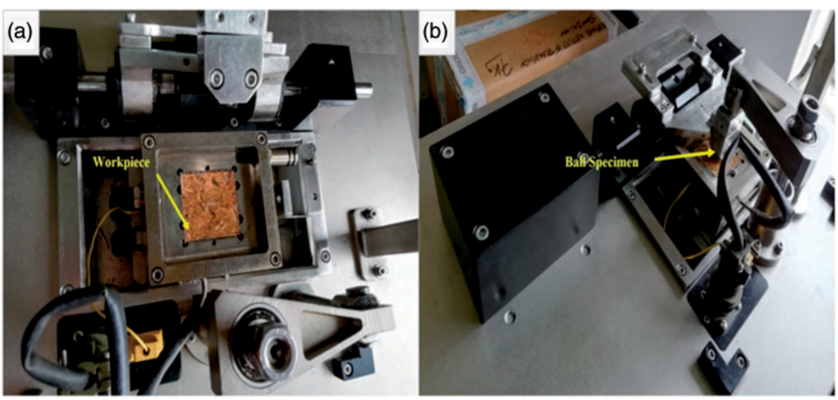


**Figure 3.** Linear reciprocating tribometer.

steel ball with a diameter of 1 cm is linearly reciprocated on the square-shaped composite specimen of size $4 \times 4 \times 0.3\,\text{cm}^3$. The experimentation was done as per ASTM G 133–05 (2016) standard [36] with an oscillating frequency and stroke length of 10 Hz and 1 cm, respectively.

Before the experiment, the ball and composite surface were properly cleaned using liquid glassware cleaner. After drying, it was again cleaned with acetone for 2 min. Then by placing it at a hot atmosphere, it was again cleaned with methanol for another 2 min. All the cleaning process were undergone with cotton swabs. In this wear testing operating parameters of load and sliding distance (SD) were varied from 5–15 N and 500–1500 m, respectively. Calculation of SD (equation (4)) and Specific Wear Rate (SWR) (equation (5)) was done using the following equations.

$$SD = 0.002 \times t \times f \times L \tag{4}$$

where, $t$ is the total time in seconds, $f$ represents the oscillating frequency used in Hz, $L$ denotes stroke length in mm.

$$SWR = \frac{WL}{\rho \times L \times SD}\,\text{mm}^3/\text{Nm} \tag{5}$$

where, $WL$ represents the change of weight in grams, $\rho$ is a density of composite specimen in g/cm$^3$, $L$ corresponds to applied load in N and $SD$ is sliding distance in m.

## SEM analysis

Scanning electron microscopy (Hitachi SU660) was used to analyze the PCF structure and the fracture surface in the wear tested composites. The scanning was carried out with a working distance of 9.2–12 mm and voltage of 15 kV. Sputter coating was provided for smooth passages of electron beam through the composite specimens.

## Taguchi optimization

Taguchi optimization technique was used to analyze the various levels of experimentation with a lesser number of trials [24]. For this four major factors influencing the wear characteristics with three levels of experiment procedure were used (Table 3). Factors such as wt.% of PF and PCF, SD from 500–1500 m and applied load from 5–15 N was used in this 27 trial Taguchi experimentation. The SWR and Coefficient of Friction (COF) were the responses for this study. All the responses were converted to Signal to Noise (SN) ratio for normalizing the results. The experiment aims to lower the SWR and COF of hybrid composites, thus smaller

**Table 3.** Factors and levels in Taguchi experimentation.

| | | Levels | | |
|---|---|---|---|---|
| Sl. No. | Factors | 1 | 2 | 3 |
| 1 | PCF wt.% | 1 | 2 | 3 |
| 2 | PF wt.% | 20 | 30 | 40 |
| 3 | Load (N) | 5 | 10 | 15 |
| 4 | Sliding Distance (m) | 500 | 1000 | 1500 |

the better ratios was used (6). Minitab-16 software tool were used for optimization [24].

$$SN = -10\log_{10}\left(\frac{1}{\mathbf{n}}\sum_{i=1}^{\mathbf{n}}\mathbf{y}_{\mathbf{i}}^{2}\right) \tag{6}$$

where, i is the experiment number, n denotes number of responses in the trial, $y_i$ represents results for ith experiment.

## Results and discussion

### PCF characterization test

The XRD results showed peaks at 14.8°, 16.1–16.17°, and 22.2–22.52° confirming the cellulose presence in PCF filler with crystallographic planes of 1–10, 110, and 200 [36] (Figure 4). The crystallinity index of 50.2, 52.74%, proved excellent crystalline property of oil cake filler after two and three hours of ball milling respectively. The peaks of 1–10 and 110 crystallographic planes almost overlapped each other in the results [32]. The crystalline size was found be 2.43 nm after 2 hours and 2.7 nm after 3 hours of ball milling. Increase in the crystalline size promotes hydrophobic nature of filler and thereby improved the bonding with matrix phases [31].

In the FTIR spectrum (Figure 5), peak at 1745 $cm^{-1}$, 1747 $cm^{-1}$ showing the uronic-ester presence with acetyl group that proved the high presence of hemicellulose, and lignin in PCF with 3 and 2 hours of ball milling [37]. The transmittance peak at 3464–3471 $cm^{-1}$ represents the presence of a lignocellulosic element with stretched vibrations in the group having –CH, –OH [32]. The peaks at 2924 $cm^{-1}$ (3 hours ball milling) and 2927 $cm^{-1}$ (2 hours ball milling), proved the existence of good cellulosic presence of –$CH_2OH$ [38]. The cellulose content in PCF was proved by the final peak at 1103–1105 $cm^{-1}$ stating asymmetric stretching [33]. All the peaks from FTIR showed the presence of cellulose, hemicellulose and lignin in PCF.

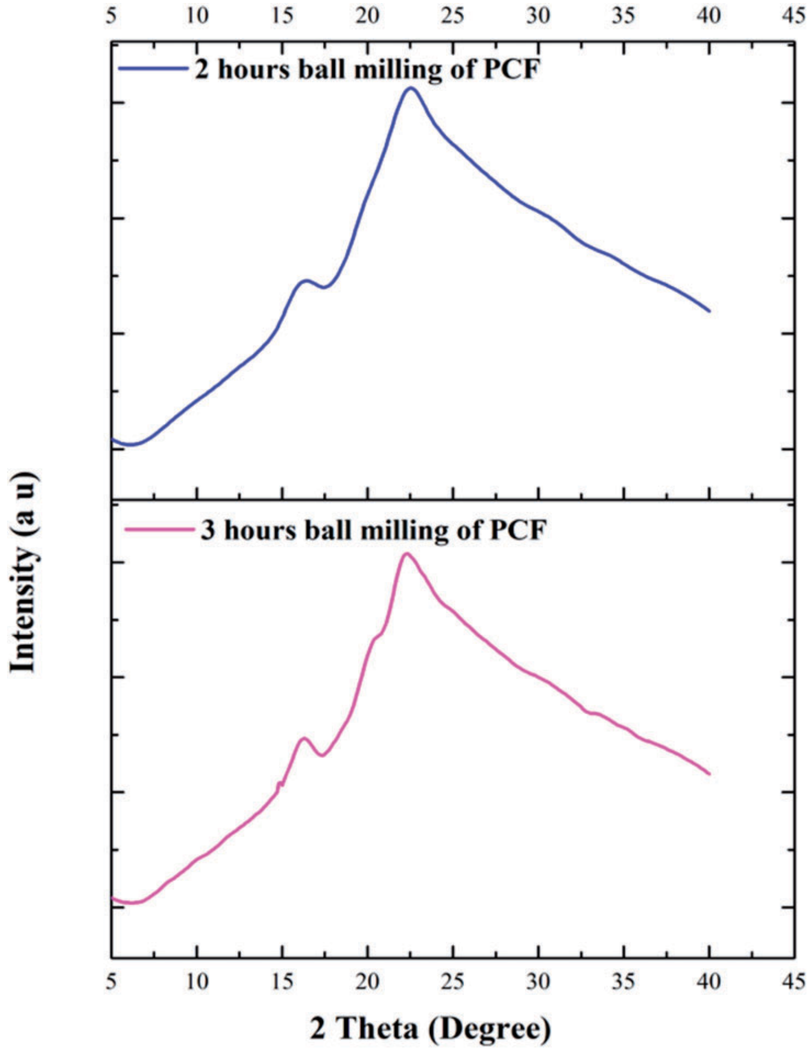


**Figure 4.** XRD results of PCF.

SEM images of PCF (Figure 6) showed a fiber-like structure surface confirming the ligno-cellulose based filler. The porous structure and even distribution of fibers were exactly visible in the oil cake filler.

## *Mechanical properties*

Mechanical results showed an enhancement in the properties with the addition of PCF. Especially, incorporation of 20 wt.% PF and 2 wt.% of PCF improved the

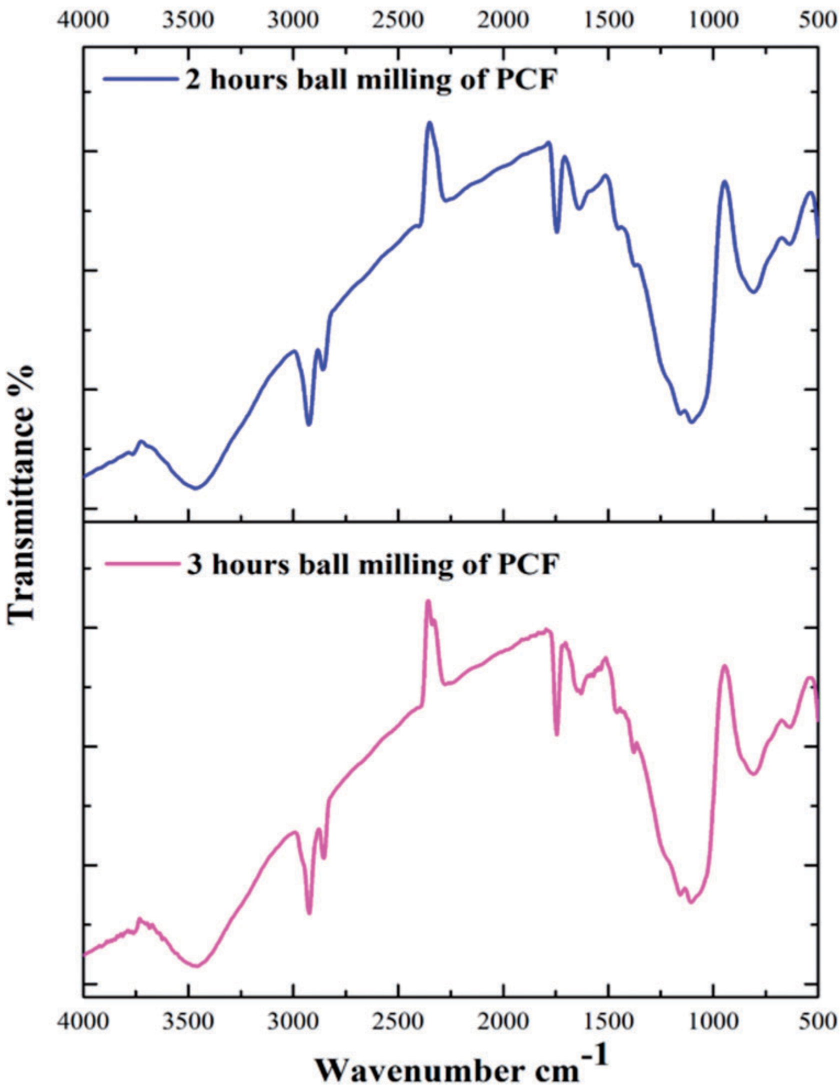


**Figure 5.** FTIR spectrum of PCF.

tensile strength (TS) from 31.25 to 37.89 MPa (Figure 7). The high incorporation of filler creates agglomeration, that declines the tensile and impact properties of natural fiber epoxy matrix composites [39,40]. Thus tensile and impact strength reduces up to 37.02 MPa and 92.24 J/m at 3 wt.% PCF substitution. Fiber reinforcement mixing at an optimum range creates a uniform dispersion in the matrix phase with better properties [41].

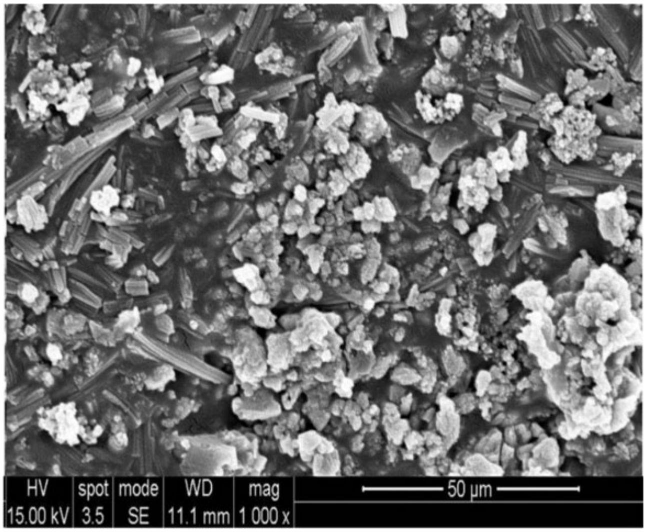


**Figure 6.** SEM image of PCF.

The HC 130 composites (Figure 8) showed a tensile, flexural, and impact strength of 27.1 MPa, 56.27 MPa, and 73.23 J/m, which was lesser when compared to HC 120 composites. The high addition of hybrid fibers created numerous surface deformations leading to property reduction [40]. Similarly, 40 wt.% PF combinations (Figure 9) give lesser properties than 20 wt.% PF, and 30 wt.% PF reinforced composites. In all the combinations of PF, PCF incorporation enhanced the TS, IS and FS of the hybrid natural fiber composites. An increase in surface area by reducing the size of filler created good bonding with hybrid fiber and epoxy resin, which improved the mechanical properties of the composites [26].

## *Water absorption results*

The addition of PCF reduced the water absorption rate of hybrid composites, while the addition of PF leads to increase in water absorption rate due to hydrophilic nature of pineapple and flax fiber was noted from Figures 10 to 12. Literature already proved that increase in fiber content resulted in higher water absorption rate [18]. Lesser adhesion of the PF fiber/matrix is the main reason for this high water absorption rate [2]. On the other hand, filler incorporation up to 2 wt.% improved the fiber/matrix bonding, which reduced the water absorption rate.

## *Taguchi analysis for SWR and COF*

In the Taguchi optimization using 27 trial (L27) experimentation (Table 4) with four factors and three-level, minimum Specific Wear Rate (SWR) of

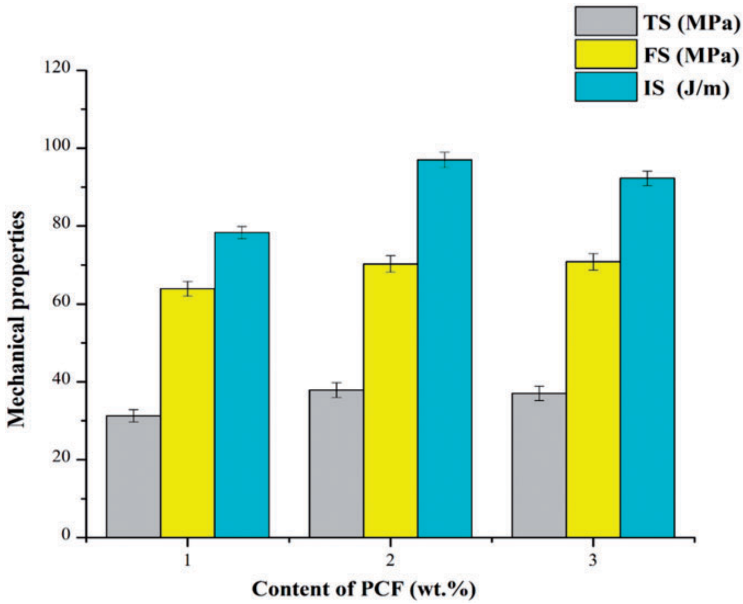


**Figure 7.** Mechanical results of PCF addition with 20 wt.% PF.

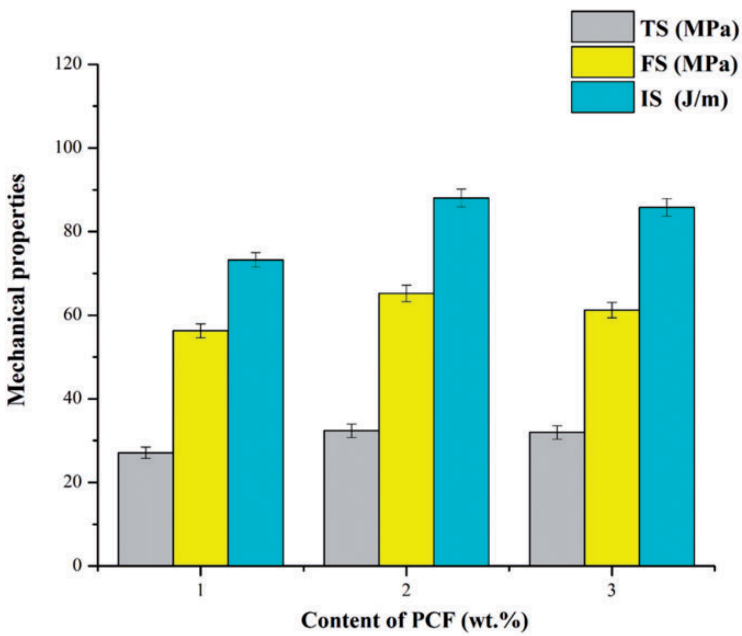


**Figure 8.** Mechanical results of PCF addition with 30 wt.% PF.

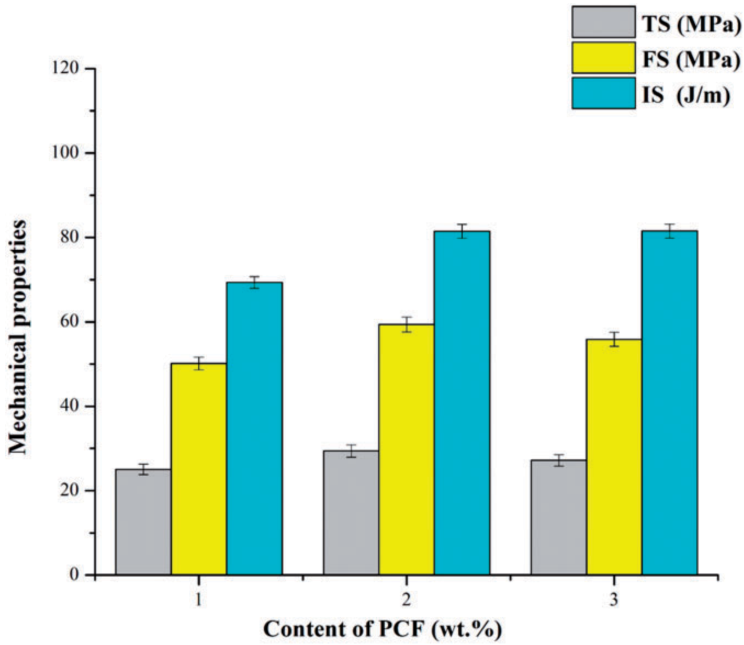


**Figure 9.** Mechanical results of PCF addition with 40 wt.% PF.

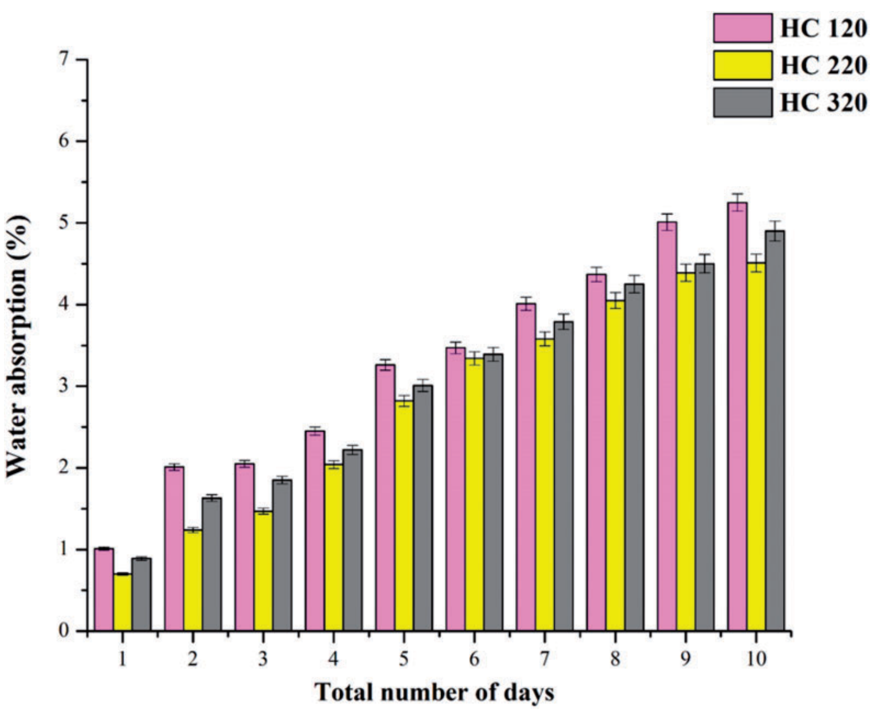


**Figure 10.** Water absorption percentage of composites with 20 wt.% PF.

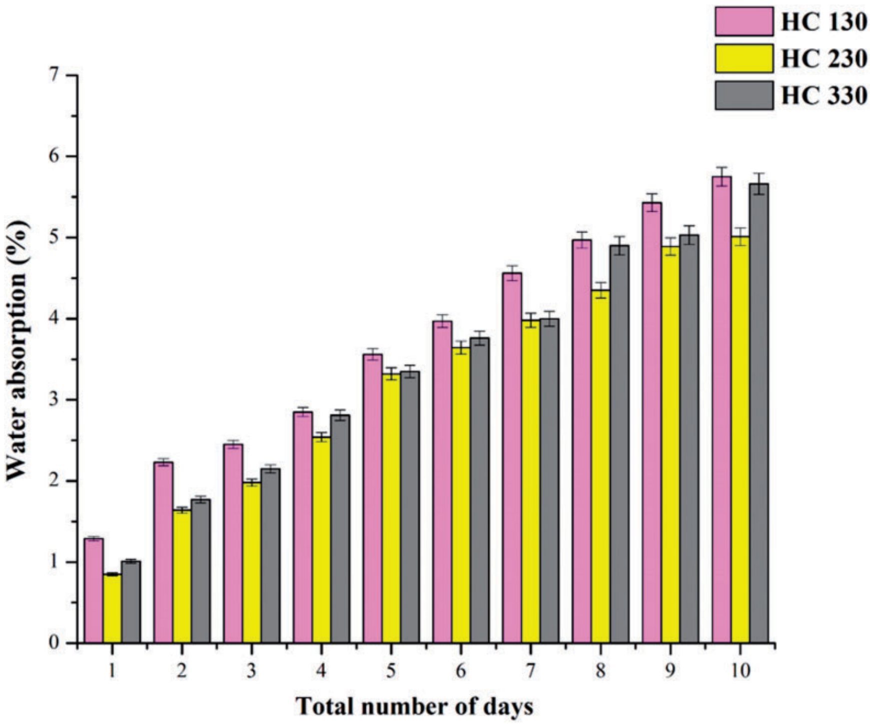


**Figure 11.** Water absorption percentage of composites 30 wt.% PF.

$3.57 \times 10^{-5}$ $mm^3/Nm$ was found in the nineteenth trial of HC320 composites with 0.5 N load and 1500 m sliding distance (SD) combination. Similarly, the maximum SWR of $37.19 \times 10^{-5}$ $mm^3/Nm$ (sixth trial) was observed in HC130 composites with 1.5 N load and 500 m SD. The next response of COF showed a minimum rate of 0.154 for HC220 composites at 1.5 N load and 500 m SD (twelfth trial). On the other hand the maximum COF was observed for HC340 composites with 1.5 N load and 500 m SD combination (twenty-seventh trial).

*SWR of hybrid composites.* The addition of PCF reduced the SWR (high SN ratio) of the hybrid composites up to 2% (Figure 13). Filler incorporation enhanced the bonding strength in the composites with good dimensional stability [25]. Filler addition above the optimum range causes agglomeration, which declines the properties of natural fiber hybrid epoxy-based composites [31]. The decrease in the size of the natural filler improved the surface area of the cellulose-based filler that adds to the compatibility of fiber and matrix phases [42]. Moreover, the filler addition improved the hardness nature of polymer composites [26] which was also an important phenomenon that improved the wear resistance of the composites.

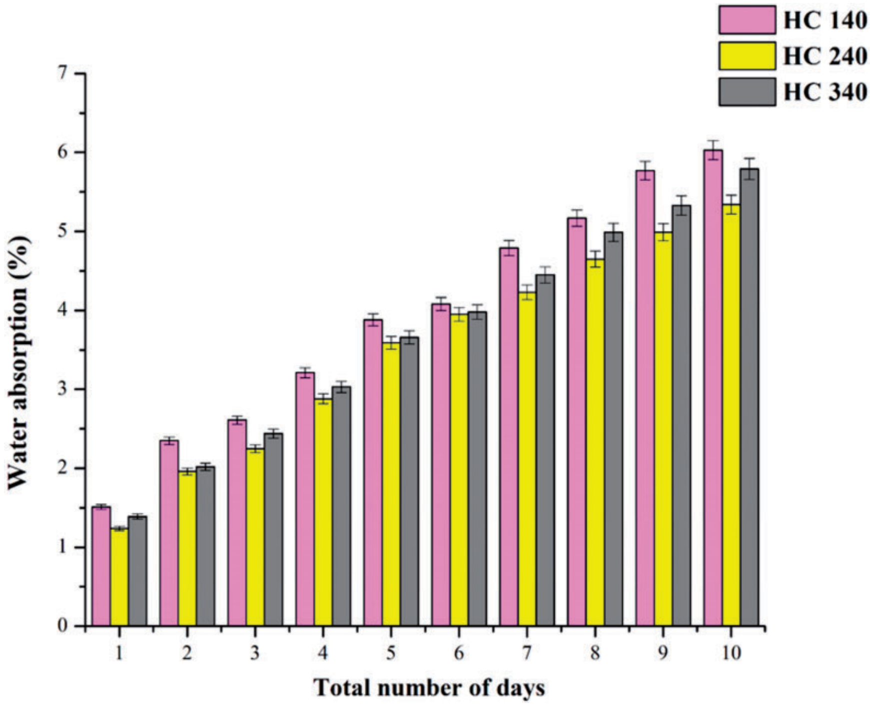


**Figure 12.** Water absorption percentage of composites with 40 wt.% PF.

Hybridization using PF fibers up to 40 wt.% showed reduced wear resistance. Fiber addition at a high percentage created an improper distribution in the polymer-based composites, which reduce the properties [40]. Furthermore, the addition of more fiber increase the surface deformations such as fiber pullouts, matrix breakages, breakage of fibers, and debonding, causing higher voids in the composites which reduced the properties [24].

Applied load from 5–15 N increased the pressure exerted on the sample which increased the wear rate [43]. The atomic force created due to the adhesion of two specimens will be much higher than materials inherent characteristics, the continuous movement of the specimen at higher load breaks, and causes wear in the composite weaker surface [18]. Furthermore, repeated passages of specimens reduced the wear rate at a higher sliding distance of 1500 m [44]. The optimized combination was found to be 2 wt.% PCF/20 wt.% PF fibers/5 N load and 1500 m SD. The good bonding of fiber reinforcement at 20 wt.% and filler at 2 wt.% with epoxy matrix, reduced the SWR of this composites.

Optimum addition of fiber reinforcement created a protective layer that prevents epoxy- based composites from wear. Film generation due to continuous movement in the composite specimen also adds to the wear resistance properties in this experimentation. Abrasive and adhesive wear was created in the

**Table 4.** Taguchi L27 orthogonal array for PF/PCF hybrid composites.

| Sl. No. | PCF | PF fiber | Load | Sliding distance | SWR ($\times 10^{-5}$) | SN ratio | COF | SN ratio |
|---|---|---|---|---|---|---|---|---|
| Units | wt % | wt % | N | m | mm$^3$/Nm | – | – | – |
| 1 | 1 | 20 | 5 | 500 | 15.43 | –23.77 | 0.164 | 15.703 |
| 2 | 1 | 20 | 10 | 1000 | 17.87 | –25.04 | 0.187 | 14.586 |
| 3 | 1 | 20 | 15 | 1500 | 19.17 | –25.65 | 0.195 | 14.196 |
| 4 | 1 | 30 | 5 | 1000 | 17.54 | –24.88 | 0.206 | 13.731 |
| 5 | 1 | 30 | 10 | 1500 | 21.76 | –26.75 | 0.221 | 13.120 |
| 6 | 1 | 30 | 15 | 500 | 37.19 | –31.41 | 0.174 | 15.207 |
| 7 | 1 | 40 | 5 | 1500 | 15.92 | –24.04 | 0.232 | 12.708 |
| 8 | 1 | 40 | 10 | 500 | 26.47 | –28.46 | 0.205 | 13.776 |
| 9 | 1 | 40 | 15 | 1000 | 29.56 | –29.41 | 0.217 | 13.290 |
| 10 | 2 | 20 | 5 | 1000 | 6.82 | –16.68 | 0.169 | 15.424 |
| 11 | 2 | 20 | 10 | 1500 | 7.80 | –17.84 | 0.183 | 14.737 |
| 12 | 2 | 20 | 15 | 500 | 24.85 | –27.91 | 0.154 | 16.230 |
| 13 | 2 | 30 | 5 | 1500 | 7.80 | –17.84 | 0.170 | 15.369 |
| 14 | 2 | 30 | 10 | 500 | 20.95 | –26.42 | 0.162 | 15.817 |
| 15 | 2 | 30 | 15 | 1000 | 25.01 | –27.96 | 0.165 | 15.647 |
| 16 | 2 | 40 | 5 | 500 | 12.67 | –22.05 | 0.212 | 13.464 |
| 17 | 2 | 40 | 10 | 1000 | 19.65 | –25.87 | 0.226 | 12.911 |
| 18 | 2 | 40 | 15 | 1500 | 22.74 | –27.14 | 0.232 | 12.708 |
| 19 | 3 | 20 | 5 | 1500 | 3.57 | –11.06 | 0.184 | 14.686 |
| 20 | 3 | 20 | 10 | 500 | 19.33 | –25.72 | 0.178 | 14.995 |
| 21 | 3 | 20 | 15 | 1000 | 14.23 | –23.06 | 0.176 | 15.090 |
| 22 | 3 | 30 | 5 | 500 | 13.97 | –22.90 | 0.194 | 14.243 |
| 23 | 3 | 30 | 10 | 1000 | 14.94 | –23.49 | 0.197 | 14.101 |
| 24 | 3 | 30 | 15 | 1500 | 24.04 | –27.62 | 0.200 | 13.960 |
| 25 | 3 | 40 | 5 | 1000 | 13.64 | –22.70 | 0.207 | 13.686 |
| 26 | 3 | 40 | 10 | 1500 | 20.47 | –26.22 | 0.229 | 12.789 |
| 27 | 3 | 40 | 15 | 500 | 30.05 | –29.56 | 0.244 | 12.238 |

polymer-based composites [16,28]. The contact between steel ball and composite specimen makes a localized bonding with them. This created a material transfer of surface from either specimen, causing wear.

The ranks were classified based on the delta values and was shown in Table 5. The difference in the lowest level reading from the highest level gives the delta value. In this experimentation, the load (ranks 1) has the most significant influence in SWR of the composites. The application of higher loads, created surface abnormalities due to the high-pressure zone created in the composite surface [45]. Fiber incorporation, sliding distance, and PCF has 2 to 4 ranks. Insufficient adhesion of reinforcement and matrix phase results in sliding of fiber during the experimentation declined the wear resistance of the composites [46]. The ANOVA results shown in Table 6 proved the significance of PCF, PF fiber, sliding distance, and

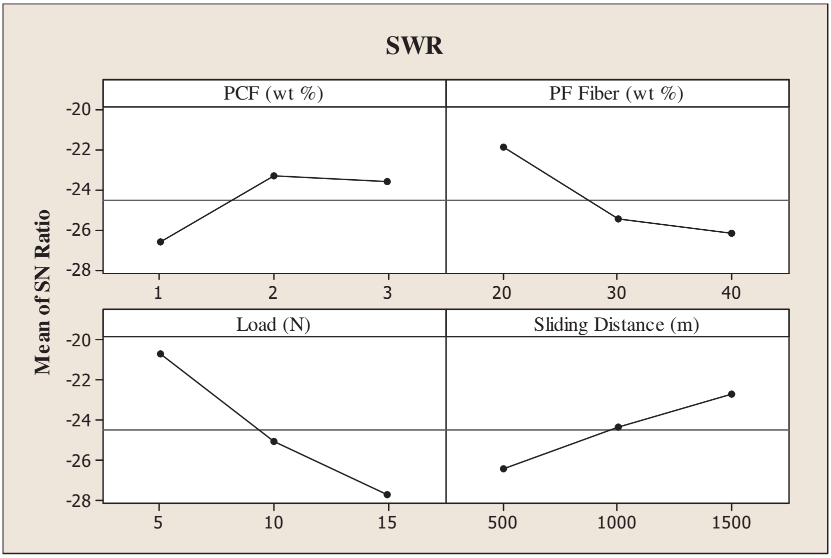


**Figure 13.** SN Ratio - SWR.

**Table 5.** Response table of SWR.

| Level | PCF | PF | Load | Sliding distance |
|---|---|---|---|---|
| 1 | –26.60 | –21.86 | –20.66 | –26.47 |
| 2 | –23.30 | –25.48 | –25.09 | –24.34 |
| 3 | –23.59 | –26.16 | –27.75 | –22.68 |
| Delta | 3.30 | 4.30 | 7.09 | 3.78 |
| Rank | 4 | 2 | 1 | 3 |

**Table 6.** ANOVA Table for SWR.

| Source | DF | Seq SS | Adj MS | F Value | P Value |
|---|---|---|---|---|---|
| PCF | 2 | 184.56 | 92.28 | 15.29 | 0.000 |
| PF | 2 | 253.78 | 126.89 | 21.02 | 0.000 |
| Load | 2 | 793.41 | 396.70 | 65.71 | 0.000 |
| Sliding distance | 2 | 196.84 | 98.42 | 16.30 | 0.000 |
| Error | 18 | 108.66 | 6.04 | | |
| Total | 26 | 1537.25 | | | |

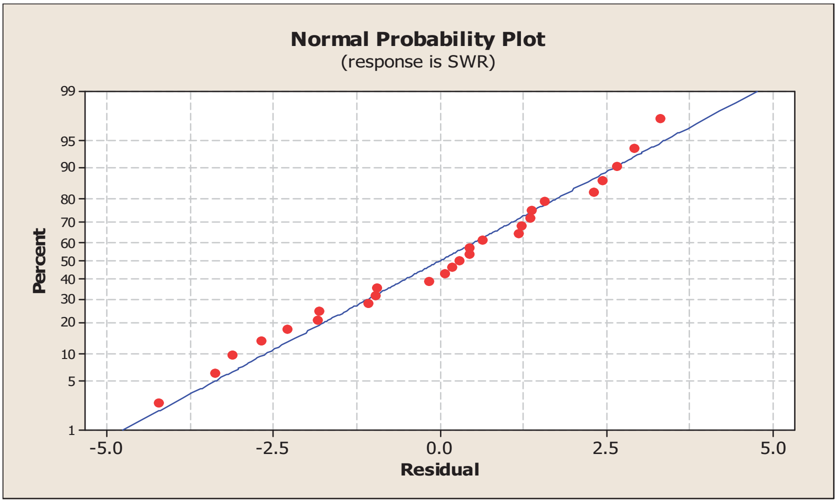


**Figure 14.** Normal probability plot for SWR.

load in this experimentation with a P value less than 0.05. Typical probability plot results (Figure 14) showed a straight line confirming this regression results can be used for predicting SWR results.

*COF of hybrid composites.* The incorporation of 2 wt.% of PCF reduced the COF (Figure 15) because the oil cake filler provides stress transferring property for the matrix and also creates good interfacial interaction with the matrix and reinforcement phase [42]. Moreover, a smooth layer will be formed due to good bonding nature in the composites which reduce the COF of the composites [35]. In addition to this the high crystalline nature of PCF created a structural enhancement in polymer-based composites. This cellulose-based filler having a single monomer unit that provides inter and intramolecular hydrogen bonding which offers a compact crystalline structure with improved adhesion property [26,30].

The addition of fiber reinforcement from 20–40% created a negative influence in COF. An increase in the fiber incorporation created an uneven distribution of reinforcement with a rough surface which result in high COF [18]. The best bonding nature was observed in the composites with 20 wt.% of PF addition (high SN ratio). Alkali treatment (5% NaOH) also provides this improved nature due to the removal of the hydroxide group from the reinforcement surface by ionizing it into alkoxide [25,40]. Moreover, the elements such as pectin, natural fats, hemicelluloses, and wax content have been reduced with the alkali treatment [35]. These all improved the compatibility of fiber/matrix phases. Applied load at 5 N showed the least COF (high SN ratio), an increase in the load created high-pressure zone in the composite target, which increase the friction [45,46]. The lowest COF was observed at sliding distance of 500m, due to the increase in the SD creating a high contact

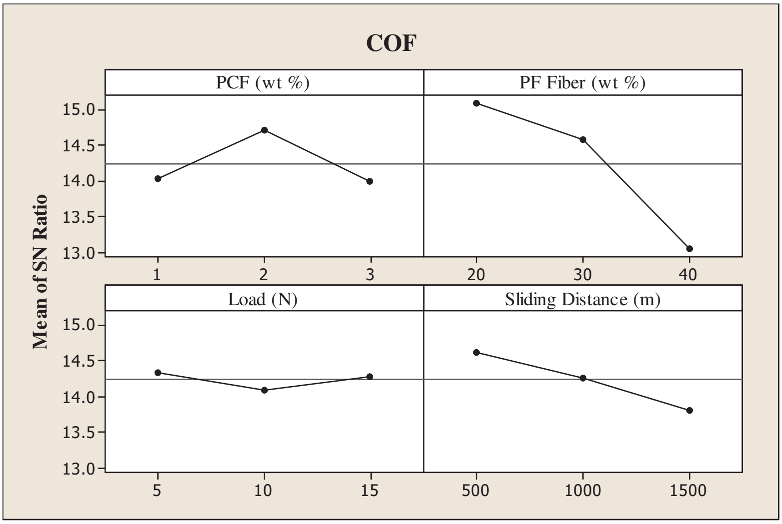


**Figure 15.** SN Ratio for COF.

**Table 7.** Response table for COF.

| Level | PCF | PF | Load | Sliding distance |
|---|---|---|---|---|
| 1 | 14.04 | 15.07 | 14.33 | 14.63 |
| 2 | 14.70 | 14.58 | 14.09 | 14.27 |
| 3 | 13.98 | 13.06 | 14.28 | 13.81 |
| Delta | 0.72 | 2.01 | 0.24 | 0.82 |
| Rank | 3 | 1 | 4 | 2 |

surface, which further increase the COF. The Taguchi results observed lower COF in HC220 at 5 N load and 500 m sliding distance.

The PF fibers have greatest influence on COF of the composites (Table 7), followed by sliding distance, PCF content, and load applied. The proper fiber addition improved the wear resistance by preventing the epoxy resin matrix from chromium steel ball direct contact. Furthermore, the ANOVA results (Table 8) proved the significance of PCF, PF fiber, and sliding distance in this experimentation with P value less than 0.05. The normal probability plot results shown in Figure 16 observed a straight line confirming this regression results can be used for predicting COF results.

## *SEM analysis after wear testing*

The SEM images of wear tested samples show the surface deformations due to operating parameters and fiber/filler additions. Figure 17(a) with 1 wt.% PCF,

**Table 8.** ANOVA table for COF.

| Source | DF | Seq SS | Adj MS | F Value | P Value |
|---|---|---|---|---|---|
| PCF | 2 | 0.0012664 | 0.0006332 | 3.56 | 0.050 |
| PF | 2 | 0.0103131 | 0.0051565 | 28.95 | 0.000 |
| Load | 2 | 0.0001379 | 0.0000690 | 0.39 | 0.684 |
| Sliding distance | 2 | 0.0014397 | 0.0007199 | 4.04 | 0.035 |
| Error | 18 | 0.0032057 | 0.0001781 | | |
| Total | 26 | 0.0163629 | | | |

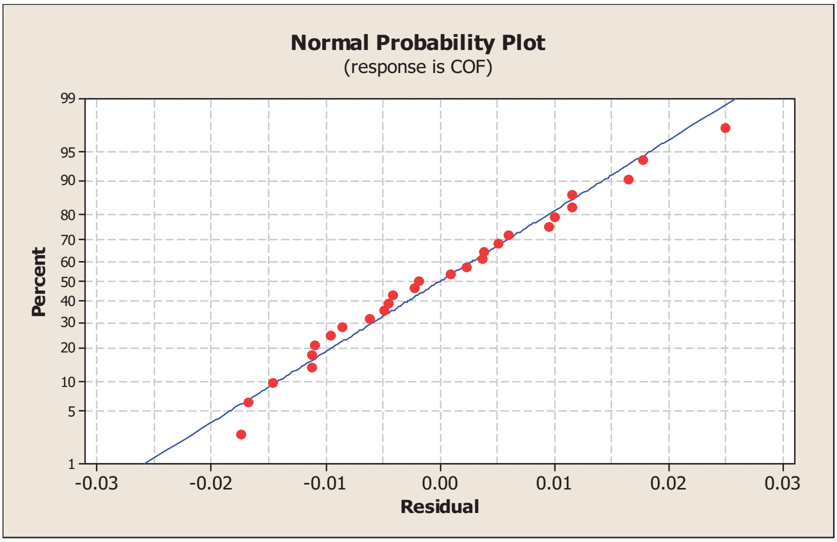


**Figure 16.** Normal probability plot for COF.

showed more surface deformations such as matrix breakages and fiber breakages. An increase in the PCF addition (2 wt. %) slightly improved the composite surfaces with lesser deformations (Figure 17(b)). Filler incorporation improved the crystalline property of the composites, thus producing a smooth layer surface, which reduces the wear rate of the composites. Filler mixing enhanced the compatibility of natural hybrid composites [25]. Tribo-layer formation (Figure 17(b)) by steel ball and natural fiber composite contact also add to the wear resistance of the polymer composites.

The fiber reinforcement (Figure 18(a)) at 20 wt.% found a small crack, small wear grooves compared to PF hybrid addition at 40 wt.% (Figure 18(b)). The reinforcement substitution of 20 wt.% also observed with a small fiber pullout. The higher fiber addition (Figure 18(b)) produced fiber debonding, deep groove formation, and matrix breakages in the polymer composites, which drastically

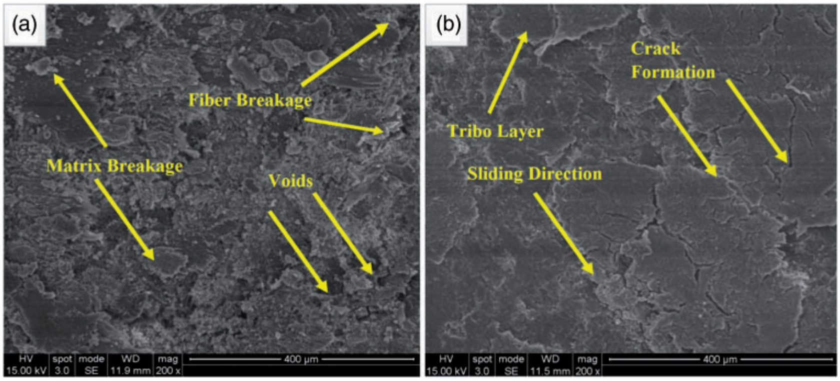


**Figure 17.** SEM results after wear testing for (a) 1 wt.% PCF, and (b) 2 wt.% PCF combinations.

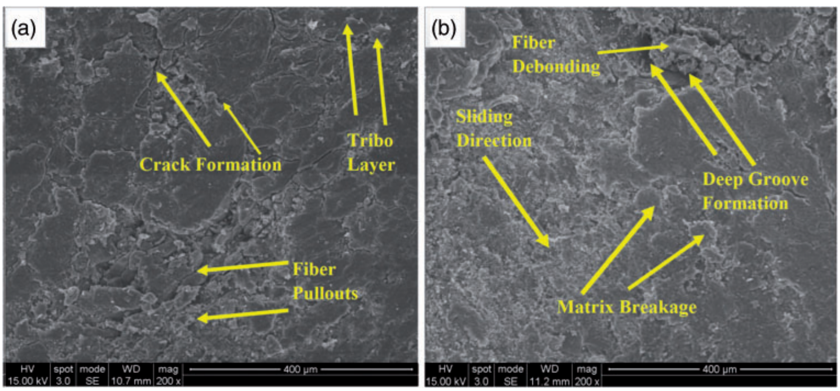


**Figure 18.** SEM results after wear testing for a) 20 wt.% PF, and (b) 40 wt.% PF combinations.

reduces the composite properties [47,48]. Moreover, higher fiber incorporation leads to uneven fiber distribution with lesser matrix/fiber compatibility [41]. This produces a rough contact surface with the linear reciprocating ball specimen that reduces the wear resistance. Fiber addition beyond the optimum range reduce the wear properties of the composites [45].

Higher load conditions (Figure 19(b)) at 15 N created substantial plastic deformation and severe damages in the surfaces compared to lower load of 5 N (Figure 19(a)) [44]. These are formed mainly due to the breakage of epoxy resin and fiber bonding at high loading. The contact surface of the counter body increase the thermal softening nature in polymer composite specimens that also enhanced the plastic deformation [47]. These high load conditions (Figure 19(b)) also increases the groove and crack formation in the natural fiber composites. The sliding distance at a high rate of 1500 m (Figure 20(b)) and 500 m SD (Figure 20(a)) does not

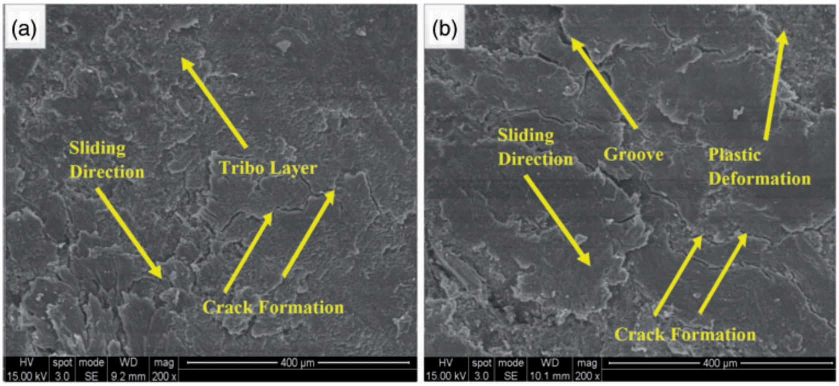


**Figure 19.** SEM results after wear testing for (a) 5 N Load, and (b) 15 N Load combinations.

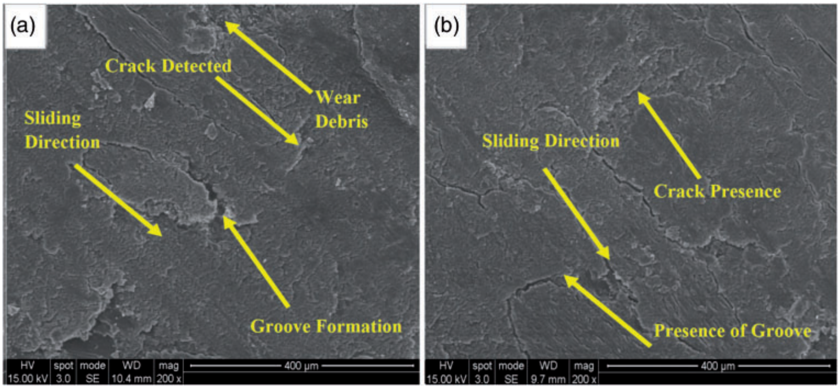


**Figure 20.** SEM results after wear testing for (a) 500 m SD, and (b) 1500 m SD combinations.

produce much fiber fractures and deformations in the composites; it is mainly due to higher wear resistance of natural fiber composites at higher sliding distance [44]. Some surface deformation such as crack, groove formation was visible in both lower and higher sliding distance combinations.

## *SEM analysis after mechanical testing*

SEM analysis after mechanical testing showed good improvement in the bonding of fiber/matrix phase by the incorporation of PCF wt.% at 3% (Figure 21(b)). In the initial PCF addition at 1 wt.% (Figure 21(a)) numerous voids and fiber breakages were directly visible, that reduces the overall properties of PF epoxy based composites. The 3 wt.% of PCF also created hackle formation in the matrix/fiber interface that also adds to the overall mechanical properties of the epoxy based

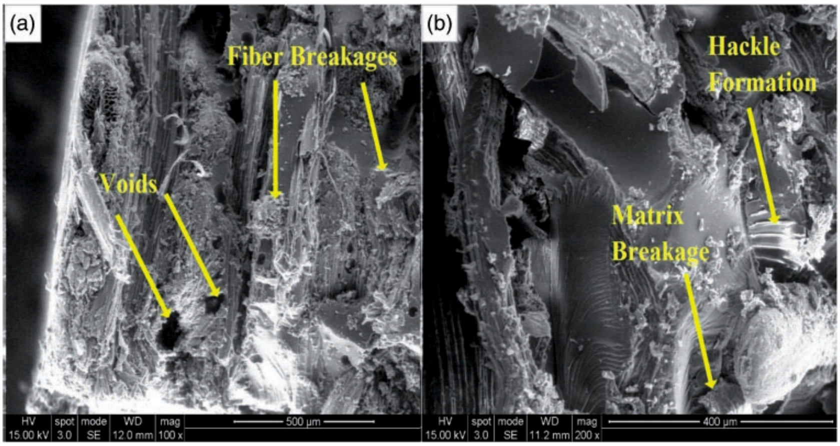


**Figure 21.** SEM analysis after mechanical testing, (a) 20 wt. % PF/1 wt.% PCF, (b) 20 wt. % PF/3 wt.% PCF combinations.

combination. Hackle formation confirms enhancement in the mechanical properties of epoxy based composites [49,50]

## Conclusions

The mechanical, water absorption and wear properties of the hybrid composites with varying load, sliding distance, filler and the reinforcement wt.% using Taguchi 27 trial combinations were investigated and observed the following results.

- The XRD and FTIR results proved the presence of lignocellulosic nature in the PCF.
- Mechanical results disclosed enhancement in the properties with the addition of PCF.
- Maximum tensile, flexural and impact properties of 37. 89 MPa, 70.28 MPa and 96.99 J/m were observed in 20 wt.% PF with PCF filler incorporation.
- The addition of more hybrid fibers created numerous surface deformations leading to property reduction.
- The Taguchi optimized specific wear rate (SWR) combination was observed with 2 wt.% PCF/20 wt.% PF fiber/5 N load and 1500 m SD while the optimized results for COF were observed in 2 wt.% PCF/20 wt.% PF/5N load/500 m SD combination.
- SEM results showed a low fracture surface in the composites having 2 wt.% of PCF. Filler incorporation improved the crystalline property of the natural fiber composites, thus producing a smooth wear debris layer surface, which reduce the wear rate of the composites.

- Fiber addition more than 20 wt.% increases the fiber/matrix bonding failure rate in composites due to uneven fiber distribution thus declining the wear applications.
- The results showed that the Pineapple/Flax natural fibers along with peanut oil cake filler could be a good alternative reinforcement material for producing friction composites for brake pad applications. Based on the encouraging results the authors has been planned to fabricate the polypropylene and polylactic acid based friction composites using these reinforcements and to study its tribological performance.

## Acknowledgements

I would like to sincerely thank Deanship of Scientific Research (DSR) at King Abdualziz University, Jeddah, Saudi Arabia for funding this project, under Grant No. (FP - 192-42). I also like to sincerely thank Science and Engineering Research Board (SERB), Govt of India, for providing me the Linear Reciprocating Tribometer facility purchased under the project ECR/2017/000839.

## Declaration of conflicting interests

The author(s) declared no potential conflicts of interest with respect to the research, authorship, and/or publication of this article.

## Funding

The author(s) disclosed receipt of the following financial support for the research, authorship, and/or publication of this article: The project was funded by the Deanship of Scientific Research (DSR) at King Abdualziz University, Jeddah, Saudi Arabia, under grant no. (FP - 192- 42).

## ORCID iDs

KR Sumesh https://orcid.org/0000-0002-9426-2372
G Rajeshkumar https://orcid.org/0000-0003-1190-2838

## References

[1] Lakshmanan A, Ghosh RK, Dasgupta S, et al. Optimization of alkali treatment condition on jute fabric for the development of rigid biocomposite. *J Ind Text* 2018; 47: 640–655.
[2] Jothibasu S, Mohanamurugan S, Vijay R, et al. Investigation on the mechanical behavior of areca sheath fibers/jute fibers/glass fabrics reinforced hybrid composite for light weight applications. *J Ind Text* 2020; 49: 1036–1060.
[3] Kumaran P, Mohanamurugan S, Madhu S, et al. Investigation on thermo-mechanical characteristics of treated/untreated *Portunus sanguinolentus* shell powder-based jute fabrics reinforced epoxy composites. *J Ind Text* 2019; 50: 1–33.

[4] Athith D, Sanjay MR, Yashas Gowda TG, et al. Effect of tungsten carbide on mechanical and tribological properties of jute/sisal/E-glass fabrics reinforced natural rubber/epoxy composites. *J Ind Text* 2018; 48: 713–737.
[5] Sanjay MR, Siengchin S, Parameswaranpillai J, et al. A comprehensive review of techniques for natural fibers as reinforcement in composites: preparation, processing and characterization. *Carbohydr Polym* 2019; 207: 108–121.
[6] Vinod A, Sanjay MR, Suchart S, et al. Renewable and sustainable biobased materials: an assessment on biofibers, biofilms, biopolymers and biocomposites. *J Clean Prod* 2020; 258: 120978.
[7] Thyavihalli Girijappa YG, Mavinkere Rangappa S, Parameswaranpillai J, et al. Natural fibers as sustainable and renewable resource for development of eco-friendly composites: a comprehensive review. *Front Mater* 2019; 6: 1–14.
[8] Rajeshkumar G. Characterization of surface modified phoenix sp. fibers for composite reinforcement. *J Nat Fib* 2020. DOI: 10.1080/15440478.2019.1711284.
[9] Rajeshkumar G. An experimental study on the interdependence of mercerization, moisture absorption and mechanical properties of sustainable phoenix sp. fibre-reinforced epoxy composites. *J Ind Text* 2020; 49: 1233–1251.
[10] Oushabi A. The pull-out behavior of chemically treated lignocellulosic fibers/polymeric matrix interface (LF/PM): a review. *Compos Part B* 2019; 174: 107059.
[11] Todkar SS and Patil SA. Review on mechanical properties evaluation of pineapple leaf fibre (PALF) reinforced polymer composites. *Compos Part B* 2019; 174: 106927.
[12] Senthilkumar K, Saba N, Chandrasekar M, et al. Evaluation of mechanical and free vibration properties of the pineapple leaf fibre reinforced polyester composites. *Constr Build Mater* 2019; 195: 423–431.
[13] Chegdani F, Wang Z, El Mansori M, et al. Multiscale tribo-mechanical analysis of natural fiber composites for manufacturing applications. *Tribol Int* 2018; 122: 143–150.
[14] Chegdani F, Mezghani S and El Mansori M. On the multiscale tribological signatures of the tool helix angle in profile milling of woven flax fiber composites. *Tribol Int* 2016; 100: 132–140.
[15] Bakare FO, Ramamoorthy SK, Åkesson D, et al. Thermomechanical properties of Bio-Based composites made from a lactic acid thermoset resin and flax and flax/basalt fibre. *Compos Part A* 2016; 83: 176–184.
[16] Nirmal U, Hashim J and Low KO. Adhesive wear and frictional performance of bamboo fibres reinforced epoxy composite. *Tribol Int* 2012; 47: 122–133.
[17] Shuhimi FF, Abdollah MF, Bin Kalam MA, et al. Tribological characteristics comparison for oil palm fibre/epoxy and kenaf fibre/epoxy composites under dry sliding conditions. *Tribol Int* 2016; 101: 247–254.
[18] Singha AS and Thakur VK. Mechanical properties of natural fibre reinforced polymer composites. *Bull Mater Sci* 2008; 31: 791–799.
[19] Mahesh V, Joladarashi S and Kulkarni SM. Physio-mechanical and wear properties of novel jute reinforced natural rubber based flexible composite. *Mater Res Express* 2019; 6: 1–19.
[20] Correa CE, Betancourt S, Vázquez A, et al. Wear performance of vinyl ester reinforced with musaceae fiber bundles sliding against different metallic surfaces. *Tribol Int* 2017; 109: 447–459.
[21] Kumar S, Patel VK, Mer KKS, et al. Himalayan natural Fiber-Reinforced epoxy composites: effect of *Grewia optiva*/*Bauhinia vahlii* fibers on physico-mechanical and

dry sliding wear behavior. *J Nat Fibers*. Epub ahead of print 20 May 2019. DOI: 10.1080/15440478.2019.1612814.
[22] Yousif BF, Lau STW and McWilliam S. Polyester composite based on betelnut fibre for tribological applications. *Tribol Int* 2010; 43: 503–511.
[23] Akpan EI, Wetzel B and Friedrich K. A fully biobased tribology material based on acrylic resin and short wood fibres. *Tribol Int* 2018; 120: 381–390.
[24] Sumesh KR and Kanthavel K. Synergy of fiber content, Al2O3 nanopowder, NaOH treatment and compression pressure on free vibration and damping behavior of natural hybrid-based epoxy composites. *Polym Bull* 2019; 77: 1–24.
[25] Sumesh KR and Kanthavel K. Effect of $TiO_2$ nano-filler in mechanical and free vibration damping behavior of hybrid natural fiber composites. *J Brazilian Soc Mech Sci Eng* 2020; 42: 1–13.
[26] Sumesh KR, Kanthavel K and Kavimani V. Peanut oil cake-derived cellulose fiber: Extraction, application of mechanical and thermal properties in pineapple/flax natural fiber composites. *Int J Biol Macromol* 2020; 150: 775–785.
[27] Joseph J, Munda PR, Kumar M, et al. Sustainable conducting polymer composites: study of mechanical and tribological properties of natural fiber reinforced PVA composites with carbon nanofillers. *Polym Technol Mater* 2020; 59: 1088–1099. DOI: 10.1080/25740881.2020.1719144.
[28] Nanda BP and Satapathy A. An analysis of the sliding wear characteristics of Epoxy-Based hybrid composites using response surface method and neural computation. *J Nat Fibers* 2020; 0478
[29] Fei J, Zhang C, Luo D, et al. Vertically aligned TiO2 nanorods-woven carbon fiber for reinforcement of both mechanical and anti-wear properties in resin composite. *Appl Surf Sci* 2018; 435: 156–162.
[30] Kumar MNS, Yaakob Z, Mohan N, et al. Mechanical and abrasive wear studies on biobased jatropha oil cake incorporated glass – epoxy composites. *J Am Oil Chem Soc* 2010; 87: 929–936.
[31] Sumesh KR, Kanthavel K and Vivek S. Mechanical/thermal/vibrational properties of sisal, banana and coir hybrid natural composites by the addition of bio synthesized aluminium oxide nano powder. *Mater Res Express* 2019; 6: 1–29.
[32] Liu Y, Lv X, Bao J, et al. Characterization of silane treated and untreated natural cellulosic fibre from corn stalk waste as potential reinforcement in polymer composites. *Carbohydr Polym* 2019; 218: 179–187.
[33] El M, Kassab Z, Aboulkas A, et al. Reuse of red algae waste for the production of cellulose nanocrystals and its application in polymer nanocomposites. *Int J Biol Macromol* 2018; 106: 681–691.
[34] Binoj JS, Raj RE and Indran S. Characterization of industrial discarded fruit wastes (*Tamarindus indica* L.) as potential alternate for man-made vitreous fiber in polymer composites. *Process Saf Environ Prot* 2018; 116: 527–534.
[35] Sumesh KR and Kanthavel K. Green synthesis of aluminium oxide nanoparticles and its applications in mechanical and thermal stability of hybrid natural composites. *J Polym Environ* 2019; 27: 2189–2200.
[36] Zhang Y, Zhang D, Wei X, et al. Enhanced tribological properties of polymer composite coating containing graphene at room and elevated temperatures. *Coatings* 2018; 8: 91.

[37] El M, Kassab Z, Barakat A, et al. Alfa fibers as viable sustainable source for cellulose nanocrystals extraction: application for improving the tensile properties of biopolymer nanocomposite films. *Ind Crop Prod* 2018; 112: 499–510.

[38] Manimaran P, Senthamaraikannan P, Sanjay MR, et al. Study on characterization of *Furcraea foetida* new natural fiber as composite reinforcement for lightweight applications. *Carbohydr Polym* 2018; 181: 650–658.

[39] Abdul Khalil HPS, M, Masri Chaturbhuj K, Saurabh, et al. Incorporation of coconut shell based nanoparticles in kenaf/coconut fibres reinforced vinyl ester composites. *Mater Res Express* 2017; 4: 1–15.

[40] Vivek S and Kanthavel K. Effect of bagasse ash filled epoxy composites reinforced with hybrid plant fibres for mechanical and thermal properties. *Compos Part B* 2019; 160: 170–176.

[41] Gupta A, Singh H and Walia RS. Hybrid filler composition optimization for tensile strength of jute fibre-reinforced polymer composite. *Bull Mater Sci* 2016; 39: 1223–1231.

[42] Sumesh KR, Kanthavel K and Kavimani V. Machinability of hybrid natural fiber reinforced composites with cellulose micro filler incorporation. *J Compos Mater* 2020; 54: 3655–3671.

[43] Aslan M, Tufan M and Küçükömeroğlu T. Tribological and mechanical performance of sisal-filled waste carbon and glass fibre hybrid composites. *Compos Part B* 2018; 140: 241–249.

[44] Maurya HO, Jha K and Tyagi YK. Tribological behavior of short sisal fiber reinforced epoxy composite. *Polym Polym Compos* 2017; 25: 215–220.

[45] Rajeshkumar G. A new study on tribological performance of phoenix sp. fiber-reinforced epoxy composites. *J Nat Fibers* 2020; DOI:https://doi.org/10.1080/15440478.2020.1724235.

[46] Rajeshkumar G. Effect of sodium hydroxide treatment on dry sliding wear behavior of *Phoenix* sp. fiber reinforced polymer composites. *J Ind Text* 2020; DOI:https://doi.org/10.1177/1528083720918948.

[47] Nirmal U, Hashim J and Megat Ahmad MMH. A review on tribological performance of natural fibre polymeric composites. *Tribol Int* 2015; 83: 77–104.

[48] Kavitha C, Hariharan V and Rajeshkumar G. Thermogravimetric analysis of *Phoenix* sp. fibre. *Adv Nat Appl Sci* 2017; 11: 53–59.

[49] Sumesh KR and Kanthavel K. Grey relational optimization for factors influencing tensile, flexural, and impact properties of hybrid sisal banana fiber epoxy composites. *J Ind Text* 2020; DOI:https://doi.org/10.1177/1528083720928501.

[50] Sumesh KR and Kanthavel K. Optimizing various parameters influencing mechanical properties of banana/coir natural fiber composites using grey relational analysis and artificial neural network models. *J Ind Text* 2020; DOI:https://doi.org/10.1177/1528083720930304.